16th World Conference on Earthquake, 16WCEE 2017
Santiago Chile, January 9th to 13th 2017
Paper N° 443
Registration Code: S-T1461199686

FAILURE TRENDS~~NUMERICAL STUDY~~ OF DOUBLE FRICTION PENDULUM BEARINGS UNDER ~~ANALYTICAL~~ PULSE EXCITATIONS

Y. Bao[(1)], T. Becker[(2)], H. Hamaguchi[(3)]

[(1)] PhD candidate, Department of Civil Engineering, McMaster University, Canada, baoy7@mcmaster.ca
[(2)] Assistant professor, Department of Civil Engineering, McMaster University, Canada, tbecker@mcmaster.ca
[(3)] Group leader, structural dynamics group, Takenaka R & D Institute, Chiba, Japan, hamaguchi.hiroki@takenaka.co.jp

Abstract

Although the global behavior of double friction pendulum bearings (DFP) has been widely studied, the failure behavior has not been significantly investigated. Understanding how and if the bearing will fail is important for both capacity based design and performance based design concepts. To look into failure, a model based on the theory of rigid body kinematics, rigid body dynamics and contact mechanics is employed with an added parallel non-linear damper with Hertz's contact law to explicitly consider the energy dissipation. Analytical Ricker pulses, including symmetric and antisymmetric Ricker pulses are selected as input excitations. For each combination of pulse amplitude and period, there are three possible outcomes for the bearing: no impact in which the bearing does not reach its maximum displacement, impact without failure in which the bearing reaches its maximum displacement limit but continues to function, and failure. These responses can be represented on an impact region spectrum, which shows that the responses tend to be continuous. The impact region spectrum can be directly used to determine the final status of the bearing when it is subjected to a Ricker pulse with specific amplitude and period. For design, Ricker pulse parameters can be extracted from site-specific pulse-type ground motions to predict the performance of the structure. However, the shape of the impact region spectrum can be influenced by different design parameters of the DFP, including radius of curvature, friction coefficient, restrainer height etc. Their influences on the shape of the impact region spectrum are investigated.

Keywords: seismic isolation; double friction pendulum bearing; impact simulation; pulse excitation; failure.

1. Introduction

Earthquake is a significant threat to our society and can cause tremendous economic losses, trigger other natural hazards, and even result casualties. In order to mitigate seismic hazard, many innovative technologies have been used in practice, and base isolation has proven to be one of the most effective ways to improve the seismic performance. Currently, there are two kinds of isolation bearings widely used in the world, rubber bearings and friction sliding bearings, and their mechanic behaviors under normal conditions are well understood. As performance based earthquake engineering moves forward, it is essential to understand their behaviors under extreme conditions, even failure. There have been several studies of failure behaviors of rubber bearings, including buckling and shear failure [1]. However, friction sliding bearings have received little study on this topic. As the configuration of the friction sliding bearings altogether different from the rubber bearings, its failure mechanism is expected to be different. More importantly, understanding the failure mechanism of friction sliding bearing is the first step to address the complex issue of collapse of isolated structures.

In this paper, a relatively simple configured friction pendulum bearing, i.e. double friction pendulum bearing (denoted as DFP hereafter) is used as an example. The basic configuration of DFP is shown in Fig. 1 below, these design parameters are provided by bearing manufacturers in Japan. The DFP is made up of two concave plates, i.e. the top plate and bottom plate and a rigid slider. Along the perimeter of the concave plate there is a restraining rim to prevent the rigid slider from moving out of place when it reaches its maximum displacement. Due to the presence of the restraining rim, a couple will develop when DFP reaches its displacement limit, depending on the amplitude of the impact, these forces will either cause the restraining rim to yield or even fracture or they may cause the rigid slider to rotate and uplift. Both scenarios can lead to the failure of the DFP. In this study, the response of the DFP is investigated under Ricker pulse excitations at first, followed by the influences of different design parameters on the failure of the DFP.

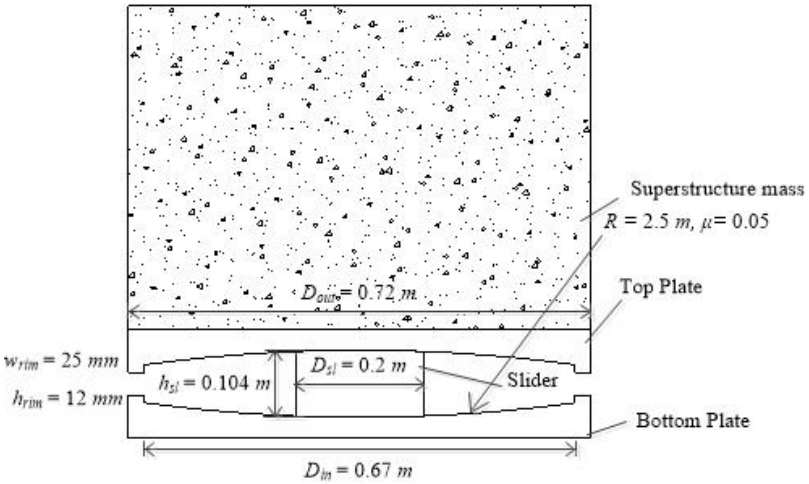

Fig. 1-Basic configuration of double friction pendulum bearing

2. Impact region spectra

A rigid body model developed by Sarlis and Constantinou [2] is used in this study to investigate the failure of the DFP. This model is based on the theory of rigid body kinematics, rigid body dynamics and contact mechanics and it can directly simulate the impact between different components and the possible uplift behaviors. This feature makes this model the ideal candidate for this research. In this model, the motion of each component is measured at its centroid, and for this study the top plate is assumed only to have horizontal and vertical translational degrees of freedom while the slider has an additional rotational degree of freedom. All of the forces (i.e. normal forces, frictional forces and potential impact forces) are concentrated ~~on~~ at the four ~~vertexes~~ vertices of the slider and the corresponding projection points on both plates. ~~In order to develop normal force and impact force in this model, small penetrations between the components are allowed and these forces are directly related to the penetration depth through the penalty stiffness.~~ However, the original rigid body model suffers from the deficiency that it cannot consider any energy dissipation during the impact because the impact force is modeled as a linear spring. To address this limitation, the Hertz's contact law in parallel with a non-linear damper [3] is added to the original rigid body model to explicitly consider the energy dissipation. In this formulation, to develop normal force and impact force in this model, small penetrations between the components are allowed and these forces are related to the penetration depth through the penalty stiffness. ~~The e~~Energy dissipation ~~is considered through a dashpot during the~~is incorporated in the approaching phase ~~within~~of an impact through viscous damping;~~,~~ the damping coefficient ~~assigned for this dashpot~~ is related to the coefficient of restitution ~~e~~, which directly reflects how much energy is dissipated during one impact. ~~In this study, a value of 0.65 is used for the coefficient of restitution.~~ A detailed description of this modified rigid body model can be found in [7].

Because of the stochastic characteristics of ground motions, it is simpler to investigate the response of the DFP under analytical pulse excitations. Here, the analytical Ricker pulses [8, 9] are used as input excitations and impact region spectra are developed to describe the response of the DFP.

The analytical Ricker pulses are selected as input excitations for two reasons. The first is that the mathematical expression is relatively simple, only two parameters (period T_p and amplitude A_p) governs its expression. The symmetric and antisymmetric Ricker pulses are expressed in Eq. (1) and Eq. (2) respectively.

$$\ddot{u}_g = A_p\left(1-\frac{2\pi^2 t^2}{T_p^2}\right)e^{-\frac{\pi^2 t^2}{T_p^2}} \tag{1}$$

$$\ddot{u}_g = \frac{A_p}{1.38}\left(\frac{4\pi^2 t^2}{3T_p^2}-3\right)\frac{2\pi t}{\sqrt{3}T_p}e^{-\frac{2\pi^2 t^2}{3T_p^2}} \tag{2}$$

where T_p is the period of the Ricker pulse, A_p is the amplitude of the Ricker pulse. The other reason is many pulse-type ground motions can be approximated by Ricker pulses, Fig. 2 below shows the 2004 Niigata ground motion in Japan, which can be represented by symmetric Ricker pulse (left side) or antisymmetric Ricker pulse (right side).

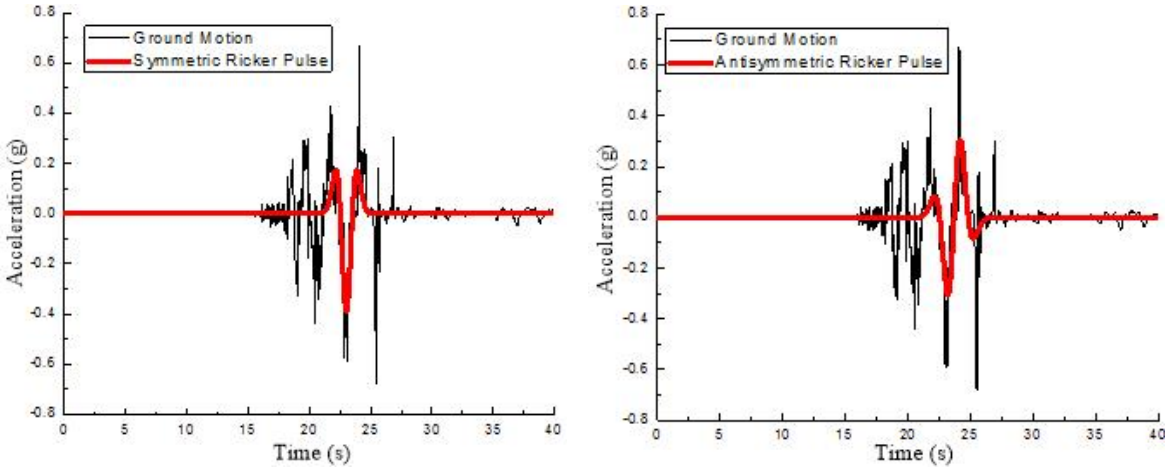

Fig. 2-Symmetric and Antisymmetric Ricker pulses

2.1 Maximum impact velocity spectra

The impact velocity spectrum, proposed by Davis [10] to describe oscillator impact, is used here to describe the response of the DFP under a specific Ricker pulse given its amplitude A_p and period T_p. All design parameters associated with the DFP are shown in Fig. 1. The impact velocity spectrum describes the relative velocity of the top plate to the bottom plate at every occurrence of an impact during a single pulse excitation. The impact velocity spectra for both symmetric and antisymmetric Ricker pulses with the same amplitude A_p = 0.8 g are illustrated in Fig. 3. The ordinate represents the relative impact velocity while the abscissa represents the frequency ratio, which is the ratio of the natural period of DFP T_b to the Ricker pulse period T_p, note for DFP T_b is a constant value (T_b = 4.5 s for R = 2.5 m) and it is expressed in Eq. (3). Each dot in the impact velocity spectrum means an impact occurs and the cross symbol indicates the failure of DFP.

$$T_b = 2\pi\sqrt{\frac{2R}{g}} \tag{3}$$

where R is the radius of curvature and g is the gravitational acceleration.

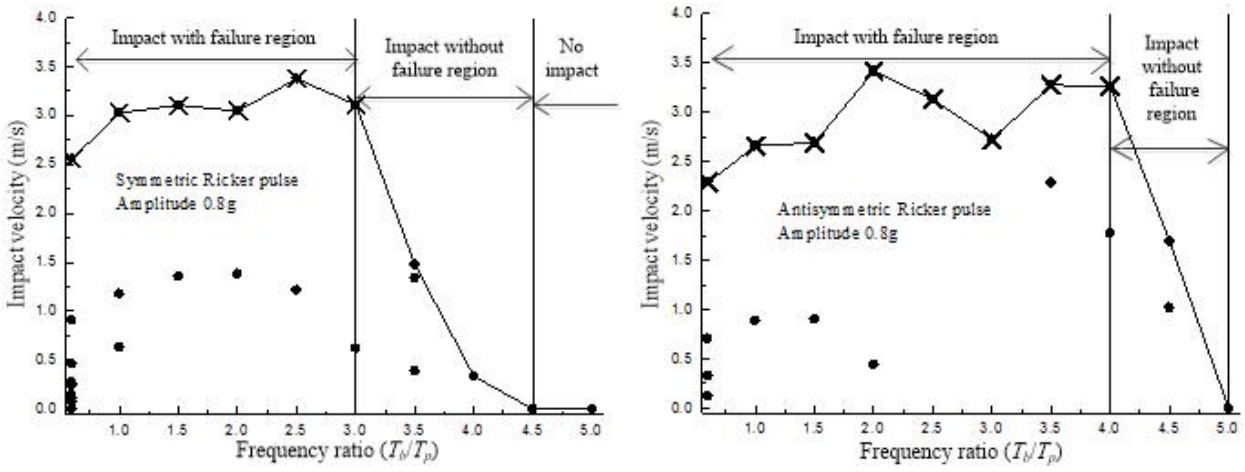

Fig. 3-Impact velocity spectra (left: symmetric, right: antisymmetric)

The impact velocity spectra provide interesting information regarding the response of DFP under a specific Ricker pulse. First of all, there may be multiple impacts that occur during one pulse excitation, for example, given the frequency ratio of 1.0, the DFP undergoes three impacts under symmetric Ricker pulse and two impacts under antisymmetric Ricker pulse. The other important observation is that even though the DFP may experience multiple impacts, not all of them will necessarily lead to the failure of DFP, only an impact with a significant velocity could result in a failure. Since in this study it is the failure of DFP of more interest, it is natural to construct the maximum impact velocity spectrum, which is similar to the concept of impact velocity spectrum, the difference is only the maximum impact velocity is plotted. The lines in Fig. 3 are the maximum impact velocity spectra for the previous Ricker pulses with the same amplitude of 0.8 g.

One more detailed maximum impact velocity spectrum for Ricker pulses with increasing amplitudes is presented in Fig. 4. One important observation of the maximum impact velocity spectra is that the frequency ratio can be divided into three different regions based on the final status of the DFP. Referring to Fig. 3, below a certain frequency ratio the impact always leads to the failure of DFP, this region is termed as the impact with failure region.

Similarly, when the frequency ratio is above a certain value, there is no impact occurring during the excitation, this region is denoted as no impact region. Between these two regions there exists an intermediate region, the impact is expected to happen but none of these impacts are at large enough velocities to cause failure. This region is termed as the impact without failure region. This phenomenon suggests the DFP is more vulnerable to long period pulses rather than short period pulses.

2.2 Impact region spectra

Based on the observation that for a single Ricker pulse amplitude, the frequency ratio can be divided into three different regions as previously described, the impact region spectrum can be derived. Unlike the impact velocity spectrum or the maximum impact velocity spectrum, the impact region spectrum directly relates the final status of DFP to the parameters of the Ricker pulses. The impact region spectrum for the baseline configuration of DFP is shown in Fig. 5, which is derived from the maximum impact velocity spectra depicted in Fig. 4. Similar to the maximum impact velocity spectrum, there are three different regions based on the final status of DFP.

Given a combination of amplitude A_p and period T_p of the Ricker pulse, it is easy to determine whether the DFP fails using these impact region spectra. For example, given a pulse-like ground motion, the analytical Ricker pulse can be extracted from the motion using wavelet analysis method. With the amplitude and period of the extracted Ricker pulse, the final status of the DFP can be directly determined by plotting the point in the impact region spectrum. Bao and Becker explored this use for a set of Japanese pulse-type ground motions [11]. This is a faster and more convenient approach compared to running a time consuming dynamic analysis. It is also a powerful tool when it comes to the preliminary design of structures isolated by DFP or evaluating the seismic performance of such isolated buildings, these applications are omitted here for brevity.

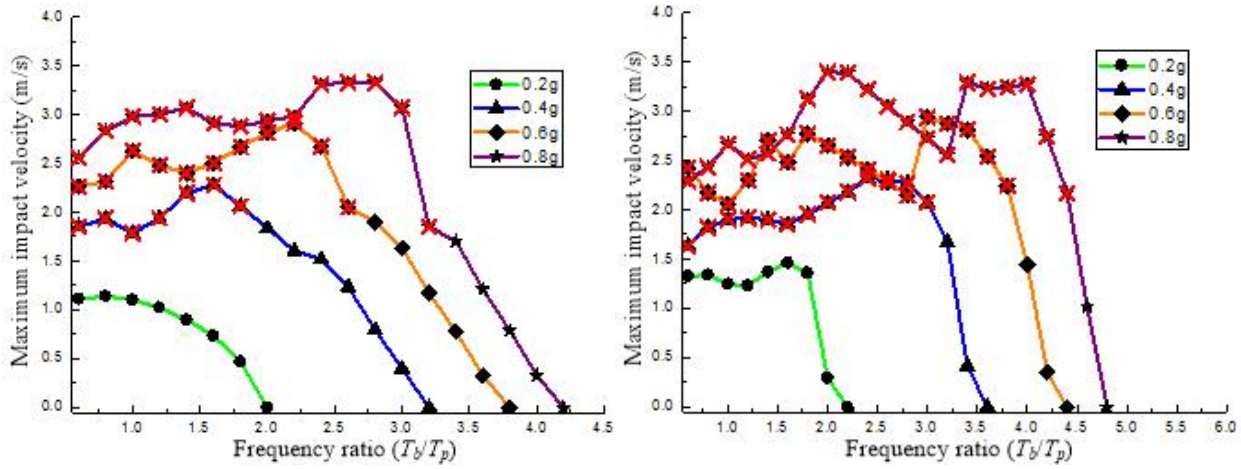

Fig. 4-Maximum impact velocity spectra (left: symmetric, right: antisymmetric)

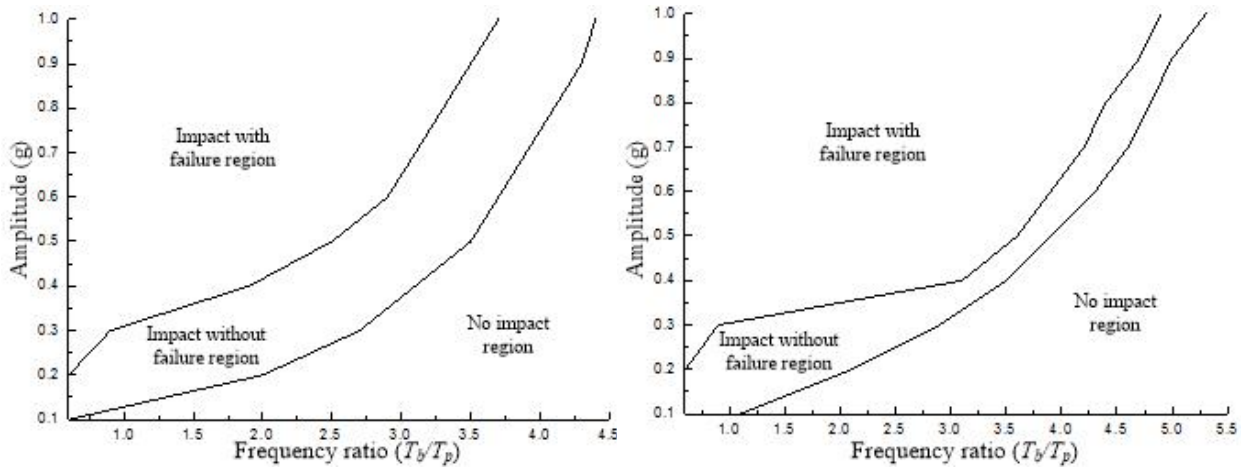

Fig. 5-Impact region spectra (left: symmetric, right: antisymmetric)

3. Influences of design parameters on impact region spectra

The impact region spectrum is fast and convenient to directly predict DFP failure. However, the impact region spectrum will be influenced by the design parameters of the DFP. In this section the influences of different design parameters on the impact region spectra will be investigated, including superstructure mass, friction coefficient, radius of curvature and restrainer height. For this parametric study, unless otherwise specified in the following sections, the baseline design values are assigned as: 1) superstructure mass resulting in 10 MPa slider pressure (32057 kg); 2) friction coefficient, μ = 0.05; 3) radius of curvature R = 2.5 m, corresponding to a period value of 4.5 s; 4) restrainer height h_{rim} = 12 mm.

3.1 Superstructure mass

In this study, the superstructure mass is assumed to be a rigid mass with its rotational degree of freedom constrained. As the rigid body model can only predict the uplift-type failures, a detailed finite element model of the DFP was created in Abaqus/Standard. The steel is assumed to have a yield stress of 345 MPa and an ultimate stress of 450 MPa with the post-yielding stiffness ratio assumed to be 0.01. Two distinct superstructure masses are used for comparison, one mass results in a slider pressure of 10 MPa and the other results in 50 MPa. Finite element analysis suggests the superstructure mass has a profound influence on the failure mechanism of DFP. When the superstructure mass is relatively small, e.g. resulting in 10 MPa in this study, the failure mechanism is controlled by the uplift behavior after the impact, as shown by the left side figure in Fig. 6; however, when the

superstructure mass is large enough, e.g. resulting in a slider pressure of 50 MPa in this study, the failure mechanism becomes the significant yielding of the restrainer rim, as shown by the right side figure in Fig. 6.

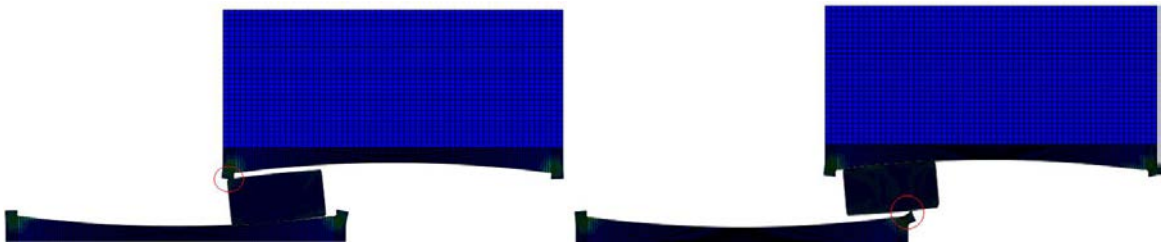

Fig. 6-Failure mechanisms of DFP (left: due to uplift, right: due to yielding)

The rigid body model described before is capable of capturing the failure mechanism due to the uplift behavior after the impact but inherently impossible to simulate the failure behavior due to yield and simulation results suggest the impact region spectrum is insensitive to the superstructure mass if the rigid body model is employed. To investigate the influence of superstructure mass on the shape of the impact region spectrum, the finite element model previously described is used and the corresponding impact region spectra are depicted in Fig. 7. Interestingly, even though the failure mechanism changes significantly when superstructure mass is different, the shape of the impact region spectra is not significantly affected. This conclusion also agrees with what is found when predicting critical pseudo acceleration values for Japanese pulse-type ground motions with different superstructure masses [11].

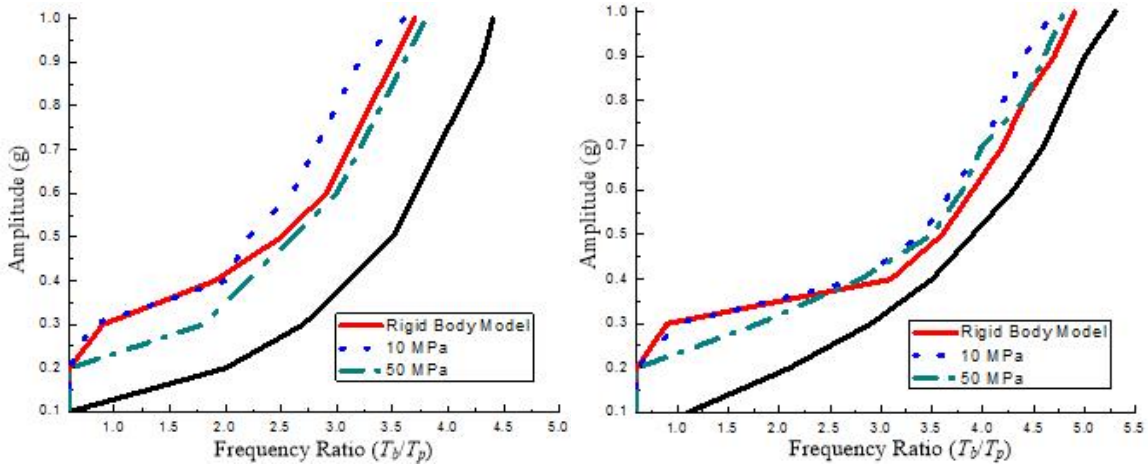

Fig. 7-Comparison of impact region spectra when superstructure mass is different (left: symmetric, right: antisymmetric)

3.2 Friction coefficient

Three different values for friction coefficient are used in this study: μ = 0.02, 0.05 and 0.08, to simplify, the dependencies on velocity, pressure and temperature are ignored in this study. The impact region spectra with different friction coefficient values are shown in Fig. 8. The influence of friction coefficient on the impact region spectra is complex: 1) For both symmetric and antisymmetric Ricker pulses, when the amplitude is low, e.g. 0.3 g in this study, increasing the friction coefficient is beneficial for avoiding both the impact and failure (note in the impact region spectra, shifting to the left side means beneficial, shifting to the right side means detrimental). 2) For symmetric Ricker pulses, when the amplitude is high, e.g. 0.9 g in this study, increasing friction coefficient is detrimental for avoiding impact but beneficial for avoiding failure. 3) For antisymmetric Ricker pulses, however, when the amplitude is high, increasing the friction coefficient is detrimental both for avoiding impact and failure.

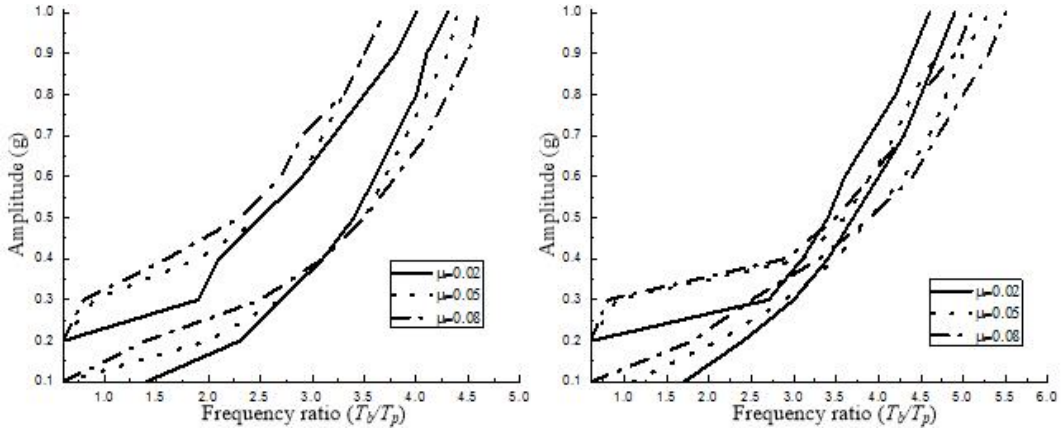

Fig. 8-Comparison of impact region spectra for different friction coefficients(left: symmetric, right: antisymmetric)

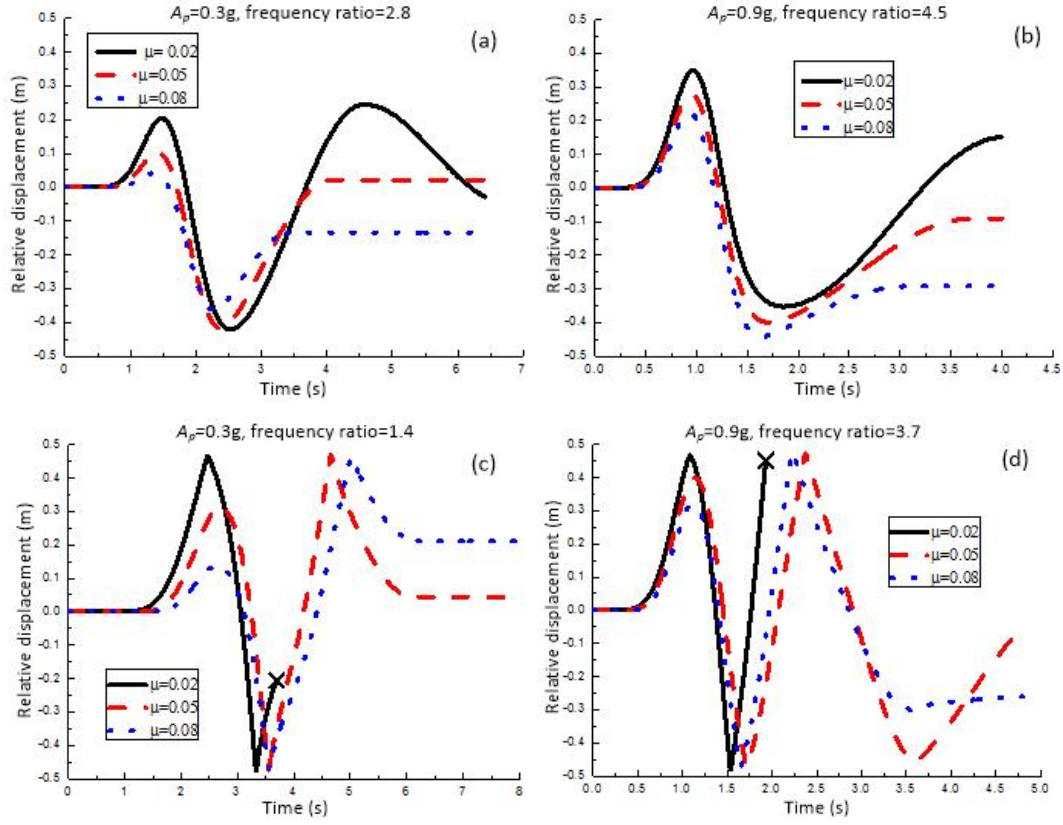

Fig. 9-Relative displacement time history under symmetric Ricker pulses

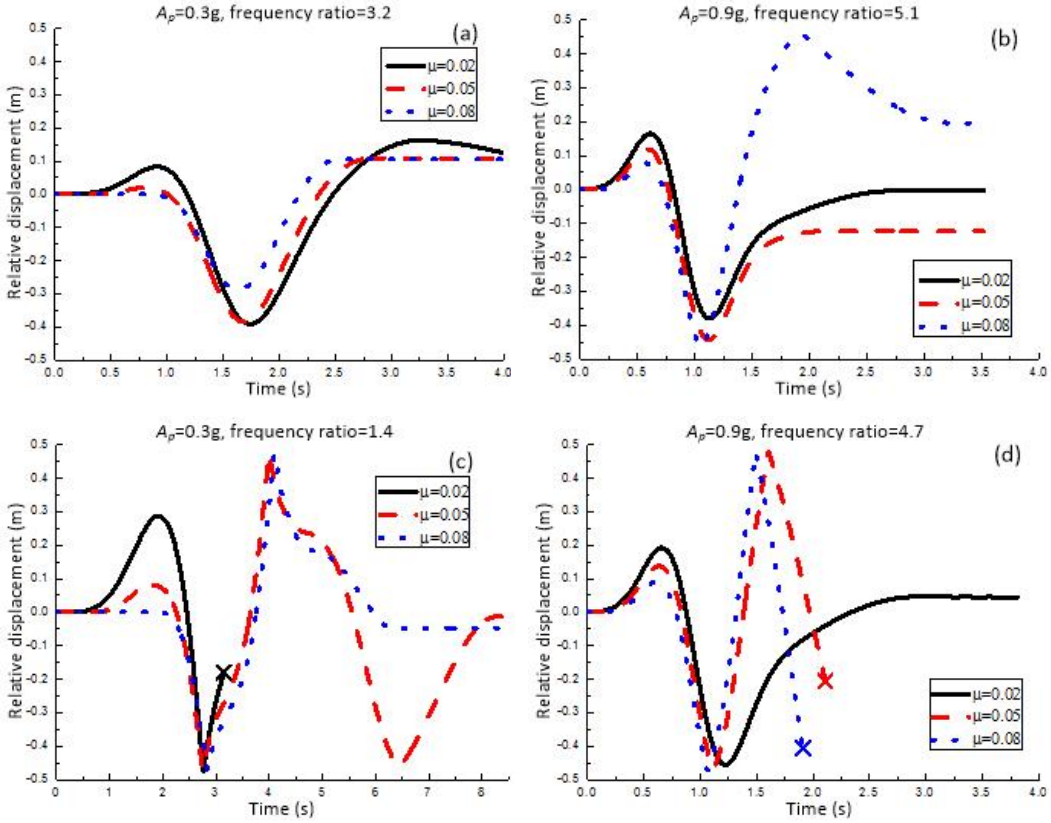

Fig. 10-Relative displacement time history under antisymmetric Ricker pulses

In order to understand how the friction coefficient affects the impact region spectra, Fig. 9 and Fig. 10 portray the horizontal displacement of the top plate relative to the bottom plate during different Ricker pulse excitations. The influence of friction coefficient on the relative displacement is quite complicated due to the nonlinear behavior of the sliding system in which the bearing equivalent period and damping changes with displacement. For both the symmetric and antisymmetric Ricker pulses, when the frequency ratio lies near the no impact region (see (a) and (b) in Fig. 9 and Fig. 10), if the pulse amplitude is low (e.g. 0.3 g in this case), decreasing the friction coefficient increases the peak displacement. On the contrary, if the pulse amplitude is large (e.g. 0.9 g), increasing the friction coefficient increases the peak displacement. This is the reason for the phenomenon that increasing the friction coefficient is beneficial for avoiding the impact at low amplitude but not at large amplitude.

For symmetric Ricker pulses, when the pulse lies within the impact without failure region (refer to (c) and (d) in Fig. 9), decreasing the friction coefficient will increase the first peak displacement until the initial impact occurs at the first peak displacement rather than the second. Due to the rebound from the first impact, the relative impact velocity at the second peak displacement is increased and therefore leads to the failure. This holds true for both low and high amplitudes when it is symmetric Ricker pulse. Thus, decreasing the friction coefficient is detrimental for avoiding failure for the symmetric Ricker pulses regardless of its amplitude.

For antisymmetric Ricker pulses, when the frequency ratio lies within the impact without failure region (refer to (c) and (d) in Fig. 10), decreasing the friction coefficient still increases the first peak displacement but it does not shift the initial impact from the second peak displacement. Therefore, the friction coefficient influences the failure region the same as the manner it does to the impact region for antisymmetric motions. Again, this complicated behavior derives from the change in the effective stiffness and equivalent damping which is highly dependent on the friction coefficient. The effective period and damping changes with the displacement of the system and with it the relationship between the bearing period and pulse period also changes.

3.3 Radius of curvature

Three different values of radius of curvature are used in this study, they are R = 2.5 m, 3.5 m and 4.5 m, which results in the natural period of DFP T_b to be 4.5 s, 5.3 s and 6.0 s. The impact region spectra using different radius of curvatures are compared in Fig. 11. Unlike other parameters discussed in this section, changing radius of curvature affects the natural period of the DFP and this in turn affects the frequency ratio in the impact region spectra. To avoid biased conclusion, the abscissa in the impact region spectra is replaced with the pulse period T_p. It is observed that changing the radius of curvature does not influence the impact region spectra significantly; only at relatively small amplitude pulse the shape of impact region spectra is affected.

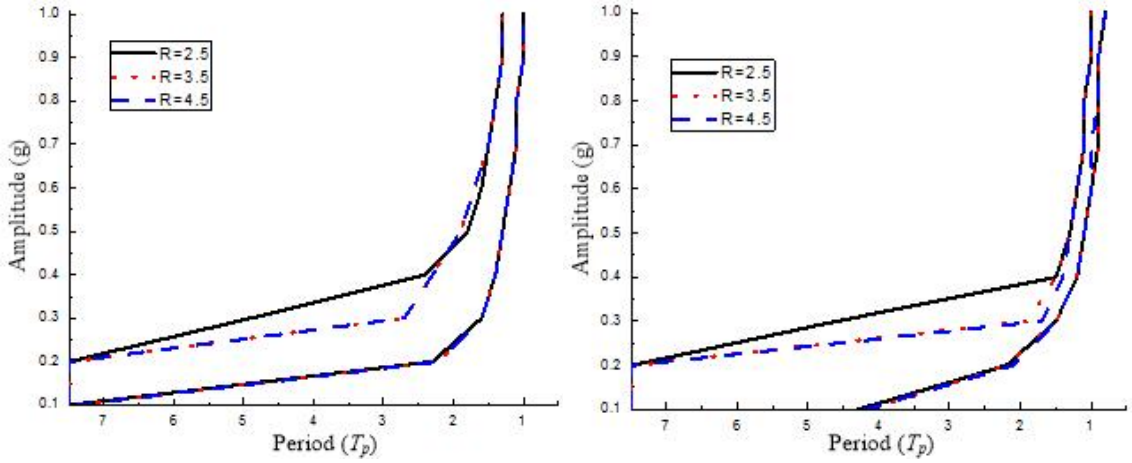

Fig. 11-Comparison of impact region spectra when radius of curvature is different (left: symmetric, right: antisymmetric)

3.4 Restrainer height

Similarly, three different values of the restrainer height are studied, they are h_{rim} = 9 mm, 12 mm and 15 mm. Intuitively, increasing the restrainer height will be beneficial for avoiding the uplift failure mechanism, however, Fig. 11 suggests changing the restrainer height has a very limited influence on the impact region spectra shape. This is because the amount of vertical displacement after the impact usually exceeds the typical restrainer height. It is expected that the restrainer height would also have minimal effect if the bearing experienced yielding-type failure.

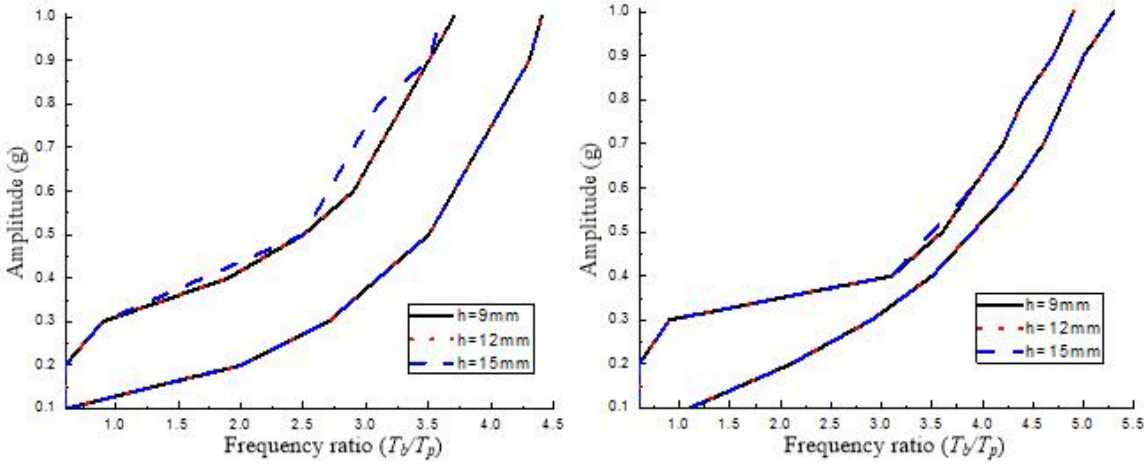

Fig. 12-Comparison of impact region spectra when restrainer height is different (left: symmetric, right: antisymmetric)

4. Conclusions

In this paper, the failure mechanism of the double friction pendulum bearing supporting a rigid mass is investigated under analytical pulse excitations. An analytical model that employs the theory of rigid body dynamics, rigid body kinematics and contact mechanics is used. The Hertz's contact law with non-linear damper in parallel is added to this model to explicitly consider the energy dissipation during impact. Ricker pulses are used as input excitations to investigate the failure of DFP due to its simple mathematical expressions. Under Ricker pulse excitations, the maximum impact velocity spectrum is developed to describe the maximum impact velocity during one specific Ricker pulse, further analysis of the maximum impact velocity spectrum shows that the frequency ratio can be divided into three regions based on the final status of the DFP. Based on this feature, the impact region spectrum is constructed and can be used for predicting the failure of DFP and preliminary design of isolated buildings.

The influence of several design parameters of the DFP on the impact region spectrum is also studied in this paper. It is found that: 1) superstructure mass has a profound influence on the failure mechanism of DFP, however, it does not significantly influence the impact region spectrum, this is a good news because the impact region spectrum can provide a relatively accurate estimation of the pulse parameters regardless of the superstructure mass. 2) The influence of friction coefficient on the impact region spectrum is complicated, it is dependent on the Ricker pulse type and the Ricker pulse amplitude. 3) The radius of curvature only has a limited influence on the shape of the impact region spectrum at low amplitude, similarly, the restrainer height has almost no influence on the impact region spectrum, this suggests that increasing the restrainer height will not be effective in terms of avoiding failure of the DFP.

5. Acknowledgements

The authors would like to express gratitude for the invaluable comments and suggestions from Dr. Masashi Yamamoto and Dr. Masahiko Higashino of the Takenaka R & D Institute.

6. References

[1] Kelly JM, Konstantinidis D (2011): *Mechanics of Rubber Bearings for Seismic and Vibration Isolation*. Wiley.

[2] Sarlis AA, Constantinou MC (2013): Model of triple friction pendulum bearing for general geometric and frictional parameters and for uplift conditions. *Technical report MCEER-13-0010*, Buffalo, NY, USA.

[3] Muthukumar S, DesRoches R (2006): A Hertz contact model with non-linear damping for pounding simulation. *Earthquake Engineering and Structural Dynamics*, 35: 811-828.

[4] Jankowski R (2005): Non-linear viscoelastic modeling of earthquake-induced structural pounding. *Earthquake Engineering and Structural Dynamics*, 34: 595-611.

[5] Jankowski R (2006): Analytical expression between the impact damping ratio and the coefficient of restitution in the non-linear viscoelastic model of structural pounding. *Earthquake Engineering and Structural Dynamics*, 35: 517-524.

[6] Jankowski R (2010): Experimental study on earthquake-induced pounding between structural elements made of different building materials. *Earthquake Engineering and Structural Dynamics*, 39: 343-354.

[7] Bao Y, Becker TC and Hiroki H (2015): Failure of double friction pendulum bearings under pulse-type motions. *Earthquake Engineering and Structural Dynamics* (accepted September, 2016).

[8] Ricker N (1944): Wavelet functions and their polynomials. *Geophysics*, 9: 314-323.

[9] Ricker N (1943): Further developments in the wavelet theory of seismogram structure. *Bulletin of the seismological society of America*, 33: 197-228.

[10] Davis RO (1992): Pounding of buildings modeled by an impact oscillator. *Earthquake Engineering and Structural Dynamics*, 21: 253-274.

[11] Bao Y, Becker TC (2016): Predicting failure in sliding isolation bearings under long period motions. *Canadian Society for Civil Engineering*. *5th International Structural Specialty Conference*, London, Ontario, Canada. June 1-4, 2016.